Climate and fire drivers of forest composition and openness in the Changbai Mountains since the Late Glacial

Article

the End User Agreement.

www.reading.ac.uk/centaur

CentAUR

Central Archive at the University of Reading

Reading's research outputs online

Climate and fire drivers of forest composition and openness in the Changbai Mountains since the Late Glacial

Meng Meng [a,b], Sandy P. Harrison [b,c], Dongmei Jie [a,d,e,f,*], Nannan Li [a], Baojian Liu [g], Dehui Li [h], Guizai Gao [a,d,e,f], Honghao Niu [a,i,**]

[a] School of Geographical Sciences, Northeast Normal University, Changchun, 130024, China
[b] Geography & Environmental Science, University of Reading, Whiteknights, Reading, RG6 6AH, UK
[c] Leverhulme Centre for Wildfires, Environment and Society, Imperial College London, South Kensington, London, SW7 2BW, UK
[d] Key Laboratory of Geographical Processes and Ecological Security in Changbai Mountains, Ministry of Education, Changchun, 130024, China
[e] Institute for Peat and Mire Research, State Environmental Protection Key Laboratory of Wetland Ecology and Vegetation Restoration, Northeast Normal University, Changchun, 130024, China
[f] Key Laboratory for Vegetation Ecology, Ministry of Education, Changchun, 130024, China
[g] HaiZhou Senior High School, Lianyungang, 222023, China
[h] College of Resources and Environment, Hebei Normal University, Shijiazhuang, 050010, China
[i] School of Archaeology, Jilin University, Changchun, 130015, China

ARTICLE INFO

ABSTRACT

Ongoing climate changes have a direct impact on forest growth; they also affect natural fire regimes, with further implications for forest composition. Understanding of how these will affect forests on decadal-to-centennial timescales is limited. Here we use reconstructions of past vegetation, fire regimes and climate during the Holocene to examine the relative importance of changes in climate and fire regimes for the abundance of key tree species in northeastern China. We reconstructed vegetation changes and fire regimes based on pollen and charcoal records from Gushantun peatland. We then used generalized linear modelling to investigate the impact of reconstructed changes in summer temperature, annual precipitation, background levels of fire, fire frequency and fire magnitude to identify the drivers of decadal-to-centennial changes in forest openness and composition. Changes in climate and fire regimes have independent impacts on the abundance of the key tree taxa. Climate variables are generally more important than fire variables in determining the abundance of individual taxa. Precipitation is the only determinant of forest openness, but summer temperature is more important than precipitation for individual tree taxa with warmer summers causing a decrease in cold-tolerant conifers and an increase in warmth-demanding broadleaved trees. Both background level and fire frequency have negative relationships with the abundance of most tree taxa; only *Pinus* increases as fire frequency increases. The magnitude of individual fires does not have a significant impact on species abundance on this timescale. Both climate and fire regime characteristics must be considered to understand changes in forest composition on the decadal-to-centennial timescale. There are differences, both in sign and magnitude, in the response of individual tree species to individual drivers.

1. Introduction

Ongoing climate change affects forest composition and structure (Searle and Chen, 2017; Hisano et al., 2018), but is also having indirect impacts on ecosystems through altering disturbance regimes (Seidl et al., 2017). Of the many climate-mediated disturbances affecting forests, including fires, windthrow, and insect and pathogen damage (Millar and Stephenson, 2015; Kulakowski et al., 2017; Willig and Presley, 2018; North et al., 2022; Hagmann et al., 2022), fires have the strongest influence on vegetation patterns and dynamics (Elvira et al., 2021). Fire plays an essential role in determining the global distribution of vegetation communities, as well as in affecting the terrestrial carbon cycle

---

(Bond et al., 2005; Fry and Stephens, 2006; Bowman et al., 2009; Prentice, 2010; Harrison et al., 2018). Forests comprise 2.3% of the global land area burnt annually and emit 5%–10% of the fire-related global greenhouse gas emissions every year (Shi et al., 2021; Scheper et al., 2021). There has been a significant increase in the frequency and severity of forest fires in many parts of the world in recent years. This has caused changes in forest composition, increased atmospheric pollution, and also resulted in significant economic losses and degradation of ecosystem services (Harrison et al., 2021). Understanding how climate and climate-induced disturbances affect forests has become a critical issue.

However, it is hard to disentangle the effects of climate and fire on forests. Modern studies can provide detailed information on post-fire changes in forest composition (e.g., Cai et al., 2013; Chen et al., 2014; Paulson et al., 2021; Andrus et al., 2022), but this information is only available for a limited number of wildfires and focuses on the short-term (decades) changes in the forest. Understanding of how fires and climate will affect forests on longer (decadal-to-centennial) timescales is limited. Sedimentary archives can provide data about climate changes, fire disturbance, and the forest response to both over many thousands of years. These long records also have the advantage of providing information about natural fire regimes, before human influence on the incidence of fire was pervasive (Sweeney et al., 2022). Statistical approaches can then be used to disentangle the influence of climate changes and fire disturbances on the observed vegetation dynamics. Generalized linear modelling is one such technique that has been widely used to investigate the relationships between predictor variables and vegetation or fire properties under modern conditions (see e.g. Bistinas et al., 2014; Lusk et al., 2018; Haas et al., 2022) because they provide highly interpretable results, can handle non-linear or non-normal relationships, and quantify the independent impact of multiple predictors even if these predictors are partially correlated with each other (Larsen and McCleary, 1972; McCullagh and Nelder, 1989; Haas et al., 2022).

In this study, we analyse palaeo-records from the Changbai Mountains, northeastern China, over the past 13,000 years to address the role of climate and fire for forest structure and composition on decadal-to-centennial timescales. Forest occupies an important position in the ecological resources of the Changbai Mountains. The absence of major fires in recent years has led to the accumulation of combustible material and increased the fire hazard. Projections of future climate change indicate significant changes in temperature and precipitation over northeastern China, with increases in mean annual temperature of more than 6 °C accompanied by increased extreme temperatures by the end of the 21st century in high-end scenarios (Yang et al., 2021; Zhu et al., 2021). Such changes will further increase the risk of wildfires. There are many peatlands in the Changbai Mountains which have been growing continuously over many millennia and thus can provide high-resolution data on climate, vegetation and fire changes through time. These resources allow us to assess the impact of climate and fires on forests on decadal-to-centennial timescales, and thus provide a scientific basis for the protection and management of the important forest ecosystems of this region.

Here, we use records from the Gushantun peatland in the Changbai Mountains and generalized linear modelling to determine which climate variables and which aspects of the fire regime have been important in affecting forest openness and the abundance of key tree species over the past 13,000 years. We address the following questions: (1) what are the climate and fire drivers that influence the density of forest cover? (2) which property of the climate or fire regime has the most impact on the forest? And (3) are there differences in the response of different tree species to climate and fire drivers?

2. Materials and methods

2.1. Regional setting and sample collection

The Gushantun (GST) peatland (42°18′22″ N, 126°16′58″ E, ~500 m

a.s.l.) is located in the west of the Changbai Mountains (Fig. 1). The peatland is nearly circular in shape with a diameter of ~1000 m and is surrounded by Cenozoic basalt of the Longgang volcanic group. The peatland has an average thickness of ~7 m and provides a sedimentary record dating back to ca 13,000 years before present (Liu, 1989; Li et al., 2017). The GST peatland is surrounded by temperate mixed conifer-hardwood forests, which are dominated by *Pinus koraiensis* and *Quercus mongolica*, together with some other broadleaved deciduous species such as *Carpinus cordata*, *Phellodendron amurense*, *Acer pictum* subsp. *Mono*, *Fraxinus mandshurica*, *Betula pendula* subsp. *Mandshurica*, *Juglans mandshurica*, *Ulmus davidiana* var. *Japonica*, *Tilia amurensis* and other conifers including *Pinus densiflora*, *Abies nephrolepis*, *Picea jezoensis* and *P. koraiensis* (Li et al., 2001; Qian et al., 2003; Stebich et al., 2009; Xu et al., 2014). The GST peatland has a temperate humid monsoonal climate today, with mean annual temperature of ~5.5 °C and mean annual precipitation of ~800 mm (Meng et al., 2020).

2.2. Generation of vegetation and fire data

2.2.1. Chronology

A 750-cm-long peat core was obtained from the GST peatland, using an Eijkelkamp peat sampler (Eijkelkamp Soil & Water, Giesbeek, The Netherlands). Fifteen bulk sediment samples were dated using accelerator mass spectrometry (AMS) ^{14}C (Meng et al., 2020) for age modelling. Here, we have recalibrated the radiocarbon ages to calendar years before present (cal yr BP) using the latest Intcal20 calibration curve (Reimer et al., 2020) implemented with the CALIB Rev.7.0.4 program (Stuiver and Reimer, 1993). The age-depth model was obtained using the Bacon v2.2 model (Blaauw and Christen, 2011). Details of the radiocarbon dates and the age-depth model are given in Appendix S1 in Supporting Information (Table S1.1, Fig. S1.1).

2.2.2. Pollen and charcoal extraction

The core was sub-sampled in the laboratory at 1-cm intervals, yielding a total of 750 samples. Pollen and charcoal particles were extracted using a modified HCl–NaOH–HF procedure (Faegri and Iversen, 1989; Zhang, 2015). Glycerine was used to prepare slides for analysis. At least 300 pollen grains were identified and counted for each sample under ×400 magnification using an Olympus microscope. The identification of pollen taxa was based on the publications of Wang et al. (1995) and Xi and Ning (1994). Trees were identified at genus level whereas most herbaceous plants were identified only to family level; Cyperaceae were excluded from the pollen sum. Charcoal particles were counted at magnifications of ×100 and ×400. Although a preliminary version of the charcoal record was previously published by Meng et al. (2020), we have increased the sampling interval from 2-cm ($n = 371$) to 1-cm ($n = 735$), providing a relatively high-resolution record with an average sampling interval of 18 years. Thus, since we are unable to track individual fire events, we focus here on decadal-to-centennial scale changes in fire regimes.

2.2.3. Reconstruction of vegetation changes

Fourteen tree species are important in the modern forest surrounding the study area. However, pollen from the genera *Carpinus*, *Phellodendron*, *Acer* and *Fraxinus* occur only rarely in the fossil samples from the GST core; these genera were therefore not considered in further analyses. The remaining 10 species in the modern forest belong to eight genera (*Abies*, *Picea*, *Pinus*, *Betula*, *Juglans*, *Quercus*, *Tilia*, *Ulmus*). We used pollen percentages of these taxa to represent their changing abundance and to reconstruct past forest composition. The ratio of arboreal to nonarboreal pollen (AP/NAP) was calculated from the pollen records to explore changes in forest openness (Favre et al., 2008).

2.2.4. Fire regime reconstruction

Fire regimes are characterised by a combination of properties, including fire size (or burnt area), intensity and frequency (Harrison
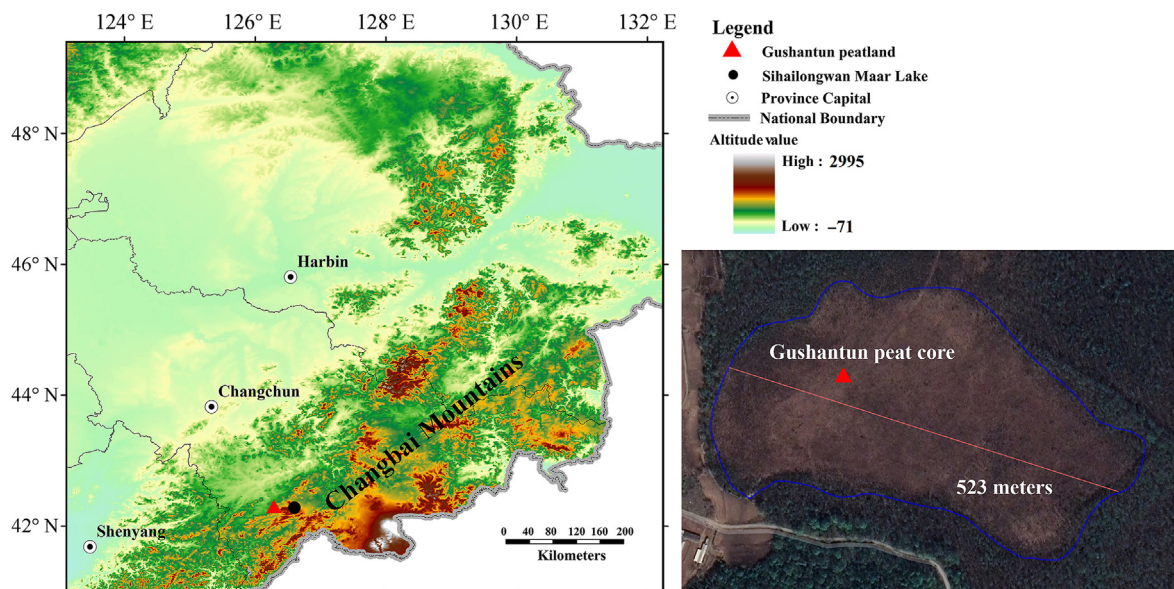
Fig. 1. Location of the Gushantun (GST) peatland site in the Changbai Mountains.

et al., 2010). Charcoal records are generally interpreted as indicators of the amount of biomass burning (e.g., Power et al., 2008; Harrison et al., 2010; Sweeney et al., 2022). However, the data can also be used to determine the background level of fire, fire frequency and magnitude using the CharAnalysis software (Higuera et al., 2009). The charcoal counts were imported into the CharAnalysis software and then converted to charcoal accumulation rates (CHAR, pieces·cm^{-2}·yr^{-1}). Prior to quantitative analysis, the CHAR values were interpolated to the median sample resolution of the profile to produce an interpolated CHAR series (Cint). A 500-year moving median was used to estimate the background component of CHAR (Cback), the low-frequency variation in CHAR which reflects changes in the rate of total charcoal production, secondary charcoal transport, and sediment mixing (Higuera et al., 2009), and the series was smoothed using locally weighted regression with a 500-year window, consistent with previous applications. The low-frequency trend was then subtracted from the CHAR to produce a residual peak CHAR series (Cpeak). Based on the assumption that the Cpeak series has two components, Cnoise (variations around Cback that reflect natural and analytical effects) and Cfire (variations exceeding variability in the Cnoise distribution) (Higuera et al., 2009), we separated Cfire from Cnoise when it exceeded the 95th percentile. Peaks passing this threshold criterion are considered to indicate major fires and used to reconstruct the fire frequency (Higuera et al., 2009). The magnitude of the charcoal peaks is assumed to represent fire severity (Higuera et al., 2014). Following Higuera et al. (2014), fire frequency was estimated as the number of charcoal peaks per 500 years (fires·500 yr^{-1}) and fire magnitude from peaks that exceed the background level (pieces·cm^{-2}·peak^{-1}). The fire events were divided into high, moderate and low magnitude/frequency intervals based on the trisection of the peak magnitude/frequency of all the reconstructions.

2.3. Statistical modelling

We used generalized linear models (GLMs) to investigate the drivers of changes in tree abundance and forest composition through the Holocene. GLMs have several advantages for this type of analysis. Firstly, they can handle non-linear or non-normal relationships between the predictors and the response variable without the need for variable transformation (McCullagh and Nelder, 1989). Secondly, they are embedded within a well-established multiple regression framework that allows the independent impact of multiple predictors to be quantified, even if they are partially correlated with each other (Larsen and McCleary, 1972). This allows the sign and the magnitude of individual predictors to be compared and thus they provide highly interpretable results. As a result of these properties, GLMs have been widely used to analyses the relationships between predictor variables and both vegetation and fire properties (Bistinas et al., 2014; Lusk et al., 2018; Haas et al., 2022). Here, in addition to the reconstructed values of CHAR, frequency and magnitude derived from the GST charcoal record, we used reconstructions of mean annual precipitation (Pann) and mean temperature of the warmest month (Mtwa) from the nearby site of Sihailongwan Maar Lake (Stebich et al., 2015). Sihailongwan Maar Lake (SHL) is only 25.4 km from the GST peatland and has the same climate; it is assumed to have experienced a similar climate evolution during the past 13,000 years. The statistical reconstructions of Pann and Mtwa exploit the multivariate nature of the pollen record (Bartlein et al., 2011) and can therefore be considered independent of the broader changes in vegetation type or openness we are seeking to explain. We investigated the correlations between the driving variables using a pairwise correlation matrix obtained from the "correlation plot" app in Origin (2022). To reduce the effects of minor fluctuations, and for consistency with the fire frequency estimates, the original data values were binned using 500-year bins with a 250-year overlap. This procedure was also applied to the AP/NAP ratios, and the pollen percentages of the eight tree taxa. We used the mean value in each overlapping bin to provide a smoothed curve of changes through time.

We created separate models for the AP/NAP ratio and each individual tree taxon. The absolute *t*-values, calculated as the fitted regression coefficient for each variable divided by its standard error, were used to assess the relative importance of each variable. Variance inflation factors (VIFs), calculated as the ratio of a coefficient in a model with multiple predictors divided by the variance of that coefficient in a single predictor model (James et al., 2013) were used to assess multi-collinearity between variables. VIF values greater than 5 are assumed to indicate excessive collinearity and are therefore excluded (O'Brien, 2007; Haas et al., 2022). Partial residual plots were constructed to demonstrate the effects of each variable with other variables held constant. The quality of models was measured by McFadden pseudo-R^2 (McFadden, 1974). The analyses were performed with the "stats", "caret", and "jtools" packages in R 4.2.2 (R Core Team, 2022).

3. Results

3.1. Reconstructions of forest dynamics

There are substantial changes in forest composition as recorded by the abundance of the main tree taxa (Fig. 2a) and forest openness as recorded by AP/NAP (Fig. 2b) during the past 13,000 years. The AP/NAP ratios (Fig. 2b) show that the forest was relatively open during the initial phase of the record and that tree abundance remained low (35.6%–89.4%, average: 69.3%) until ca 8.4 cal kyr BP. Tree cover increased after 8.4 cal kyr BP, but fluctuated considerably. Multi-centennial intervals of relatively open forest occurred ca 5.7–5.1 cal kyr BP and 3.5–2.5 cal kyr BP. Forest cover increased after 2.5 cal kyr BP and was relatively constant until ca 0.3 cal kyr BP when it declined.

In terms of composition changes, the forest was dominated by *Betula* before 12.0 cal kyr BP, and the abundance of *Abies* and *Picea* was higher than during later periods. Between 12.0 and 10.8 cal kyr BP, *Betula* decreased rapidly and *Ulmus* became dominant. *Pinus* also increased significantly at this time. Broad-leaved trees were generally more abundant than conifers between 10.8 and 5.0 cal kyr BP, and the abundance of

all taxa was relatively stable except for brief, large increases in *Betula* occurring around 8.5–5.5 cal kyr BP. All the broad-leaved trees decreased in abundance after ca 5.0 cal kyr BP, while the coniferous trees (especially *Pinus* and *Abies*) increased in importance. *Pinus* showed the most pronounced increase, reaching maximum percentages (47.2%) between 2.0 and 0.5 cal kyr BP.

3.2. Reconstructions of fire regimes

There were large changes in CHAR (Fig. 2c), magnitude (Fig. 2d) and frequency (Fig. 2e) during the past 13,000 years. Between 13.0 and 11.5 cal kyr BP, the record indicates the study area was characterised by high frequency but low magnitude fires. The early Holocene (11.5–10.0 cal kyr BP) was characterised by a high frequency of severe fires. Between 10.0 and 8.5 cal kyr BP, the frequency of fires decreased significantly and the magnitude was also lower. During the middle and late Holocene (8.5 cal kyr BP to the present), the general level of fire was relatively low but there were short-lived intervals of increased frequency at ca 8.2–7.9, 7.1–6.9, 5.5–5.0, and 2.6–1.5 cal kyr BP, and intervals of higher magnitude fires at ca 8.2, 6.1, and from 1.0 cal kyr BP to the present.
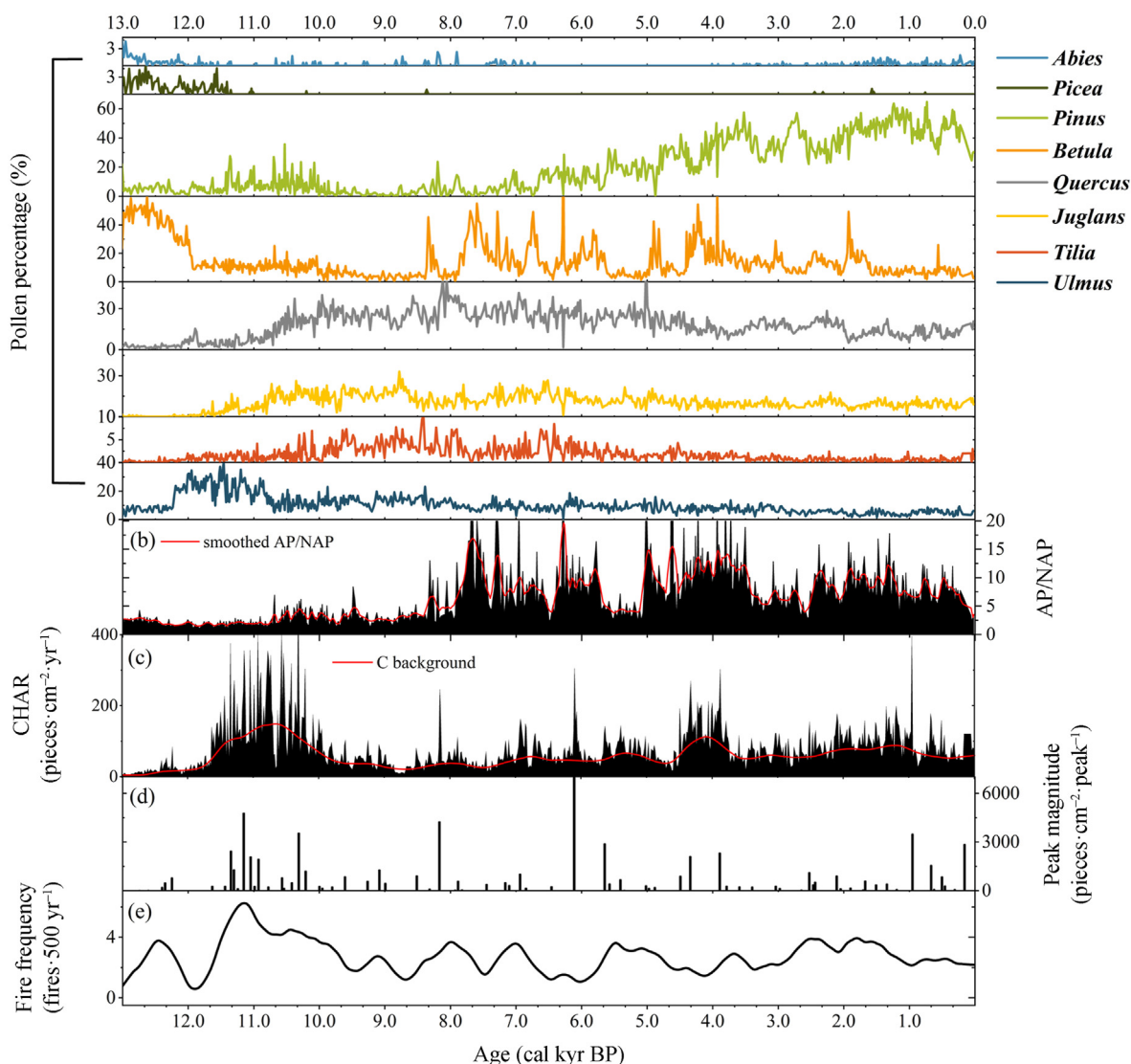
Fig. 2. Reconstructed vegetation dynamics and fire regimes for Gushantun (GST) peatland profile over the past 13,000 years. (**a**) Pollen percentages of individual tree taxa; (**b**) the ratio of arboreal to non-arboreal (AP/NAP) pollen; (**c**) interpolated records of charcoal accumulation (CHAR) (Cint) (pieces·cm^{-2}·yr^{-1}) with background CHAR (Cback) indicated by the red line; (**d**) fire magnitude indicated by peak magnitudes (pieces·cm^{-2}·peak^{-1}); (**e**) fire frequency indicated by values of Cpeak per 500 years (fires·500 yr^{-1}). (For interpretation of the references to colour in this figure legend, the reader is referred to the Web version of this article.)

3.3. Statistical analyses of the drivers of forest changes

The pairwise correlation matrix (Fig. 3) indicated that Pann and Mtwa have a significant positive relationship (coefficient = 0.64, $p \leq$ 0.001), which is consistent with the temperate monsoon climate of the study area with simultaneous wetting and warming. CHAR has a significant positive relationship with frequency (coefficient = 0.59, $p \leq 0.001$) and magnitude (coefficient = 0.45, $p \leq 0.001$). Fire frequency has a significant negative correlation with precipitation (coefficient = −0.36, $p \leq 0.05$), the more frequent fires occurred in drier periods. There are no significant correlations between other variables. Despite the significant relationships between some of the variables, the VIF values are all <5 (Table 1) indicating that the impact of collinearity on the GLM models is small except in the case of *Picea*. The VIF values in *Picea* model are all higher than 5, and all variables are eliminated. The McFadden pseudo-R^2 values for individual models ranged from −0.02 to 0.55 (Table 1). The low (and negative) values for the *Betula* ($R^2 = 0.00$) and *Abies* ($R^2 = −0.02$) models indicate that these models do not explain the observed variation in the response; values between 0.2 and 0.6 are generally considered to indicate a good model (McFadden, 1974).

The number of significant variables varied between the nine models (Table 1). Pann was the only significant variable influencing forest openness, with a strong positive relationship (*t*-value = 6.47) to AP/NAP (Figs. 4a and 5a). Frequency (*t*-value = −2.02) was the only significant variable in the *Betula* model, and had a significant negative relationship with the abundance of this taxon (Figs. 4c and 5d). Two variables were retained in the *Abies*, *Quercus* and *Juglans* models. Mtwa (*t*-value = −2.68) and CHAR (*t*-value = −2.06) were both negatively related to the abundance of *Abies* (Figs. 4b and 5b). Mtwa (*t*-value = 8.06) has a significant positive relationship with the abundance of *Quercus* but CHAR (*t*-value = −4.54) had a negative effect (Figs. 4d and 5e). Mtwa (*t*-value = 5.90) also had a positive effect on the abundance of *Juglans*, while Pann had a negative effect (*t*-value = −2.48) (Figs. 4e and 5f). Three variables were retained in the *Pinus* and *Ulmus* models. Pann (*t*-value = 10.17) and frequency (*t*-value = 2.54) were positively related to the abundance of *Pinus* (Figs. 4d and 5c), and only Mtwa (*t*-value = −8.59) showed a negative relationship (Figs. 4d and 5d). In the *Ulmus* model, Mtwa (*t*-value = 2.21) showed a positive relationship, while both Pann (*t*-value = −8.20) and frequency (*t*-value = −2.41) showed negative relationships with abundance (Figs. 4h and 5h). Four variables were retained in the *Tilia* model: Mtwa (*t*-value = 10.10) showed a positive relationship with
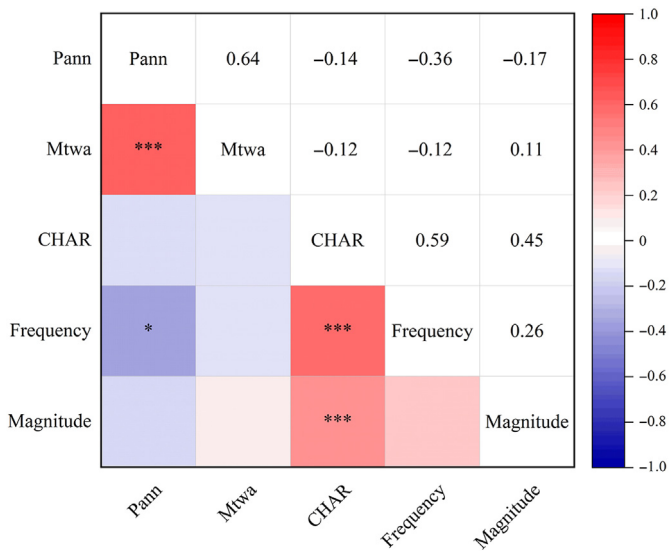
Fig. 3. Pairwise correlation matrix between the predictor variables, where the significance values are indicated by stars (***$p < 0.001$, **$p < 0.01$, and × $p < 0.05$).

Table 1
Summary statistics with regression coefficients, *t*-values and variance inflation factors (VIF) for the generalized linear models including all variables. Significance values are indicated for each variable where ***$p < 0.001$, **$p < 0.01$, and × *$p < 0.05$.

Predictors	AP/NAP			Abies			Picea			Pinus		
	Coefficient	t-value	VIF	Coefficient	t-value	VIF	Coefficient	t-value	VIF	Coefficient	t-value	VIF
(Intercept)	−7.77**	−3.35		1.45	1.26		—	—		1.10	0.91	
Pann	0.01***	6.47	1.29	0.00	1.09	2.88	—	—	—	0.02***	10.17	3.30
Mtwa	−0.01	−0.15	1.37	−0.20*	−2.68	2.97	—	—	—	−0.65***	−8.59	2.93
CHAR	0.01	1.04	1.90	−0.01*	−2.06	2.92	—	—	—	0.00	0.70	1.72
Frequency	−0.18	−0.85	1.79	0.44	1.81	2.37	—	—	—	0.47*	2.54	1.71
Magnitude	0.00	0.12	1.35	0.00	0.16	1.69	—	—	—	0.00	1.02	1.47
Pseudo-R^2 (McFadden)	0.34			−0.02			—			0.55		

| Predictors	Betula			Quercus			Juglans			Tilia			Ulmus		
	Coefficient	t-value	VIF	Coefficient	t-value	VIF	Coefficient	t-value	VIF	Coefficient	t-value	VIF	Coefficient	t-value	VIF
(Intercept)	−1.81	−1.51		−6.54***	−6.61		−4.86***	−4.53		−4.71***	−5.14		4.40***	4.06	
Pann	−0.00	−0.13	2.30	−0.00	−1.61	2.02	−0.00*	−2.48	2.31	−0.01***	−8.18	3.01	−0.01***	−8.20	2.53
Mtwa	0.04	0.69	2.03	0.34***	8.06	1.54	0.32***	5.90	1.92	0.54***	10.10	2.45	0.12*	2.21	2.04
CHAR	0.01	1.61	1.95	−0.01***	−4.54	2.08	−0.00	−0.34	2.08	−0.01*	−1.86	2.43	0.00	0.39	3.04
Frequency	−0.35*	−2.02	1.88	0.15	1.32	2.20	−0.05	−0.30	2.08	−0.58***	−3.98	2.66	−0.41*	−2.41	3.19
Magnitude	−0.00	−0.87	1.35	0.00	0.24	1.45	−0.00	−1.13	1.46	0.00	0.20	1.47	0.00	1.30	1.42
Pseudo-R^2 (McFadden)	0.00			0.36			0.23			0.48			0.38		
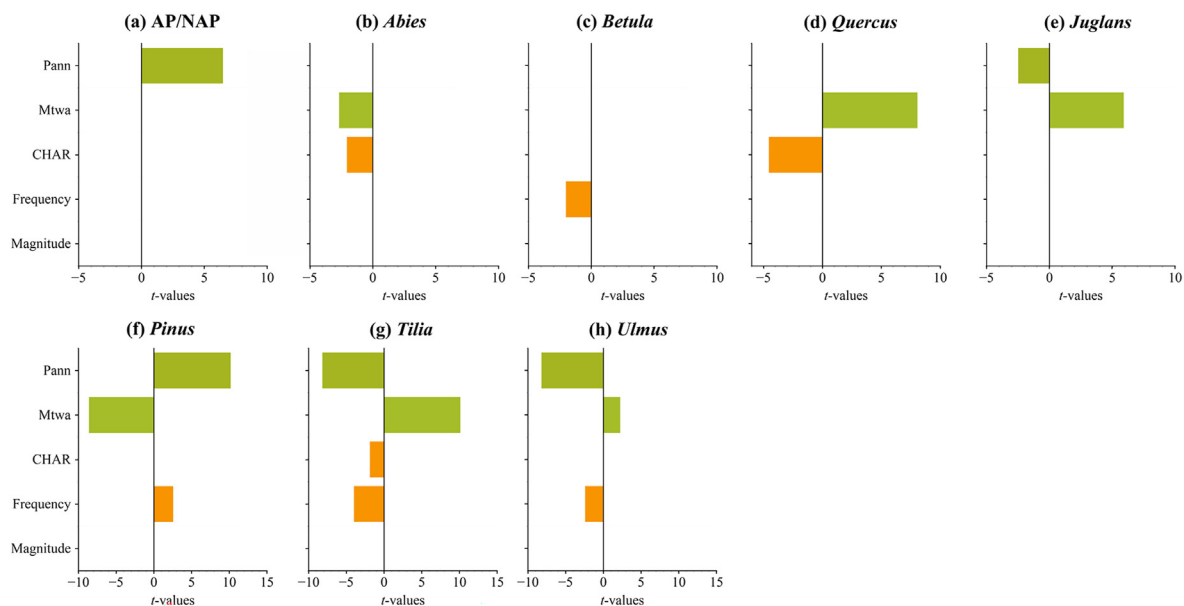
Fig. 4. *t*-values for each significant predictor variable. Climate variables are shown in green and fire variables in orange. Note that the scales differ between the upper plots and the lower plots. (For interpretation of the references to colour in this figure legend, the reader is referred to the Web version of this article.)

the abundance of this taxon, while Pann (*t*-value = −8.18), frequency (*t*-value = −3.98), and CHAR (*t*-value = −1.86) showed negative correlations (Figs. 4g and 5g).

The effects of the five variables differed between the models (Fig. 4). The climate variables were more important than the fire variables, except for *Betula* which showed no strong climate influence. The negative relationship between the abundance of *Abies* and *Pinus* with summer temperature is expected because these are relatively cold-tolerant taxa. Similarly, the positive relationship between summer temperature and the abundance of *Quercus*, *Juglans*, *Tilia* and *Ulmus* is expected since these are more warmth-demanding taxa. Annual precipitation is less important than summer temperature for most of the tree taxa, except for *Pinus* and *Ulmus*. However, precipitation is the only driver of forest openness as measured by AP/NAP; AP/NAP ratios showed a significant positive correlation with precipitation indicating that forests became more closed when precipitation levels were higher. However, the relationship between taxon abundance and annual precipitation is negative (when significant) except in the case of *Pinus*. Although temperature and precipitation were correlated (Fig. 3), they have opposite effects on most taxa.

Fire variables had no significant effect on forest openness or on the abundance of *Juglans*. CHAR was significantly negatively correlated with the abundance of *Abies*, *Quercus*, and *Tilia*. Fire frequency had a significant negative relationship with *Betula*, *Tilia* and *Ulmus*, but was positively related to the abundance of *Pinus*. Fire magnitude was not significant in any of the models. Since both fire frequency and fire magnitude were derived from CHAR, we tested whether the lack of relationship with magnitude (and the sign of the relationships with frequency) was affected by the inclusion of CHAR as a predictor by constructing models using only four variables after removal of CHAR (Table S1.2, Figs. S1.2 and S1.3). Removing CHAR resulted in no variable being significantly related to the abundance of *Betula*, whereas in the full model this taxon was sensitive to fire frequency. However, removing CHAR did not affect the significance or sign of the relationships in the other models. Fire magnitude remained unimportant for explaining changes in either forest openness or taxon abundance.

4. Discussion

Changes in precipitation drives forest openness at the GST site, with increasing precipitation leading to more dense closed forests. This

finding is consistent with previous studies where forest expansion has been closely linked to increased moisture availability and open woodlands were favoured by arid climates (Connor et al., 2013; Kuneš et al., 2015). The major increase in forest cover at the GST site occurred around 8.0 cal kyr BP, and high AP/NAP ratios remained generally high until the late Holocene. The timing of this initial increase in forest is consistent with records from several other sites in the Changbai Mountains (Fig. 6), as is the high tree cover until the late Holocene (Yuan and Sun, 1990; Jiang et al., 2008; Yu et al., 2008; Liu et al., 2009; Stebich et al., 2015; Xu et al., 2019), indicating that the increased precipitation was a regional feature presumably reflecting the orbitally-induced expansion of the East Asian monsoon in northern China during the middle Holocene (Liu et al., 2015; Zhou et al., 2016; Li et al., 2018).

Forest composition, as reflected by changes in the abundance of individual taxa, is influenced by climate but summer temperature changes generally have a larger impact than changes in moisture. Previous studies in the Changbai Mountains suggest that changes in forest composition are largely driven by temperature changes (Xu et al., 2014; Gao et al., 2018). The response to summer temperature, which has a significant negative effect on conifer trees like *Abies* and *Pinus,* and a significant positive effect on broad-leaved trees including *Quercus*, *Juglans*, *Tilia* and *Ulmus*), is consistent with the general understanding of their temperature tolerances (Harrison et al., 2010), results from modern pollen and vegetation surveys (Zheng et al., 2008), and observed changes in response to recent warming (Wang et al., 2013). The relationships with precipitation, however, are not consistent with the known moisture preferences of individual species since precipitation had a significant negative relationship with *Juglans*, *Tilia*, *Ulmus* and a significant positive relationship with *Pinus*. It seems probable that, despite the significance of these relationships and the low VIFs obtained for the models, these counter-intuitive results reflect an inherent correlation between summer temperature and monsoon rainfall over the Holocene. The strongly positive relationship between moisture and the abundance of *Pinus,* which is the dominant species through the middle and late Holocene, likely reflects the significant positive correlation between precipitation and forest closure as indicated by the AP/NAP ratio.

Zheng et al. (2018) have made reconstructions of mean annual air temperature (Maat) at GST peatland based on the distribution of bacterial branched glycerol dialkyl glycerol tetraethers (brGDGTs). Analyses of modern data from the Jingyu meteorological station, which is close to the GST peatland, indicate that there is a significant positive correlation
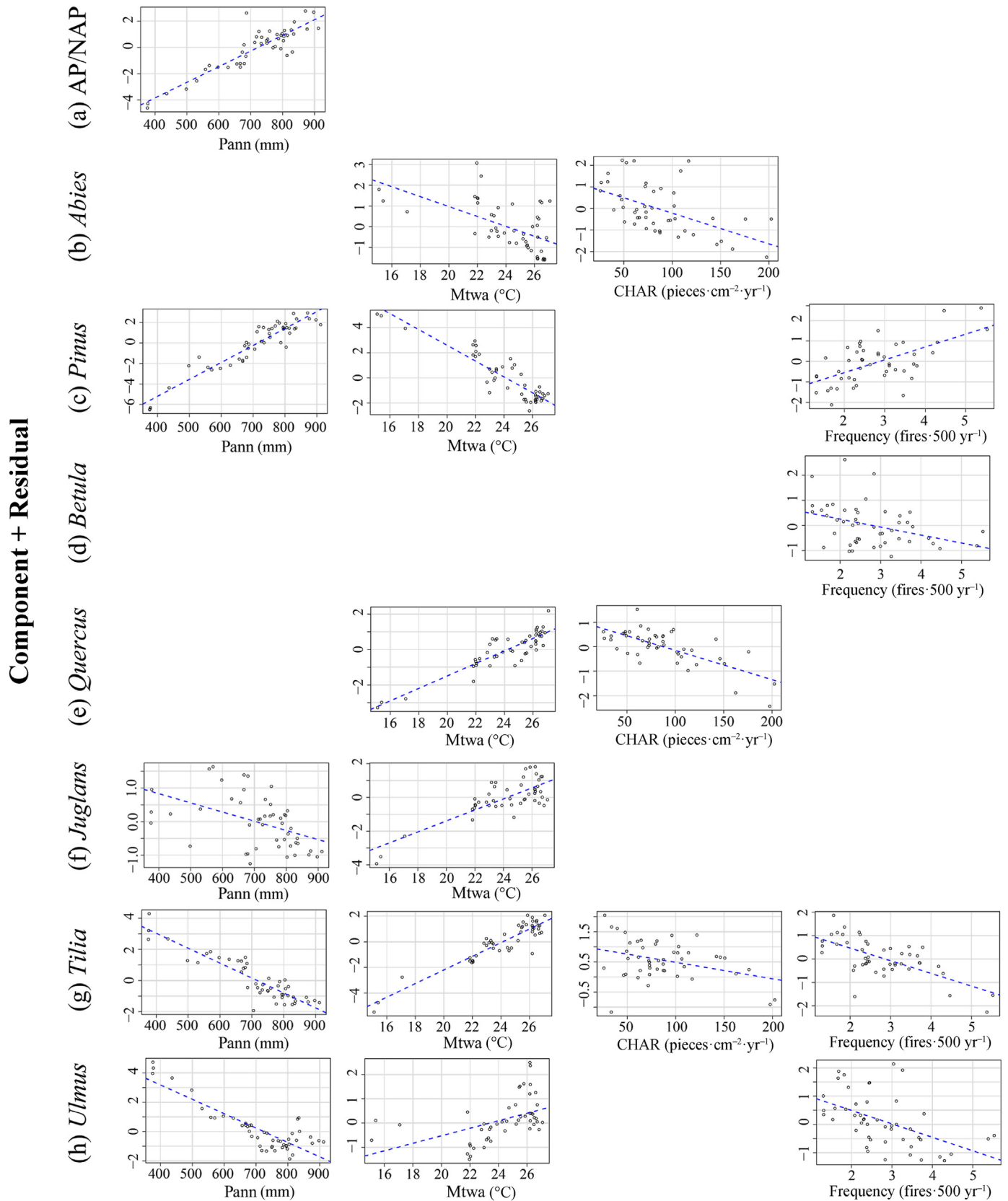
Fig. 5. Partial residual plots for the ratio of arboreal to non-arboreal (AP/NAP) pollen and 8 tree taxa as functions of annual precipitation (Pann, mm), mean temperature of the warmest month (Mtwa, °C), charcoal accumulation (CHAR, (pieces·cm^{-2}·yr^{-1}) and frequency (fires·500 yr^{-1}). Blue lines show the expected residuals if the relationship between predictor and response variable was linear. (For interpretation of the references to colour in this figure legend, the reader is referred to the Web version of this article.)
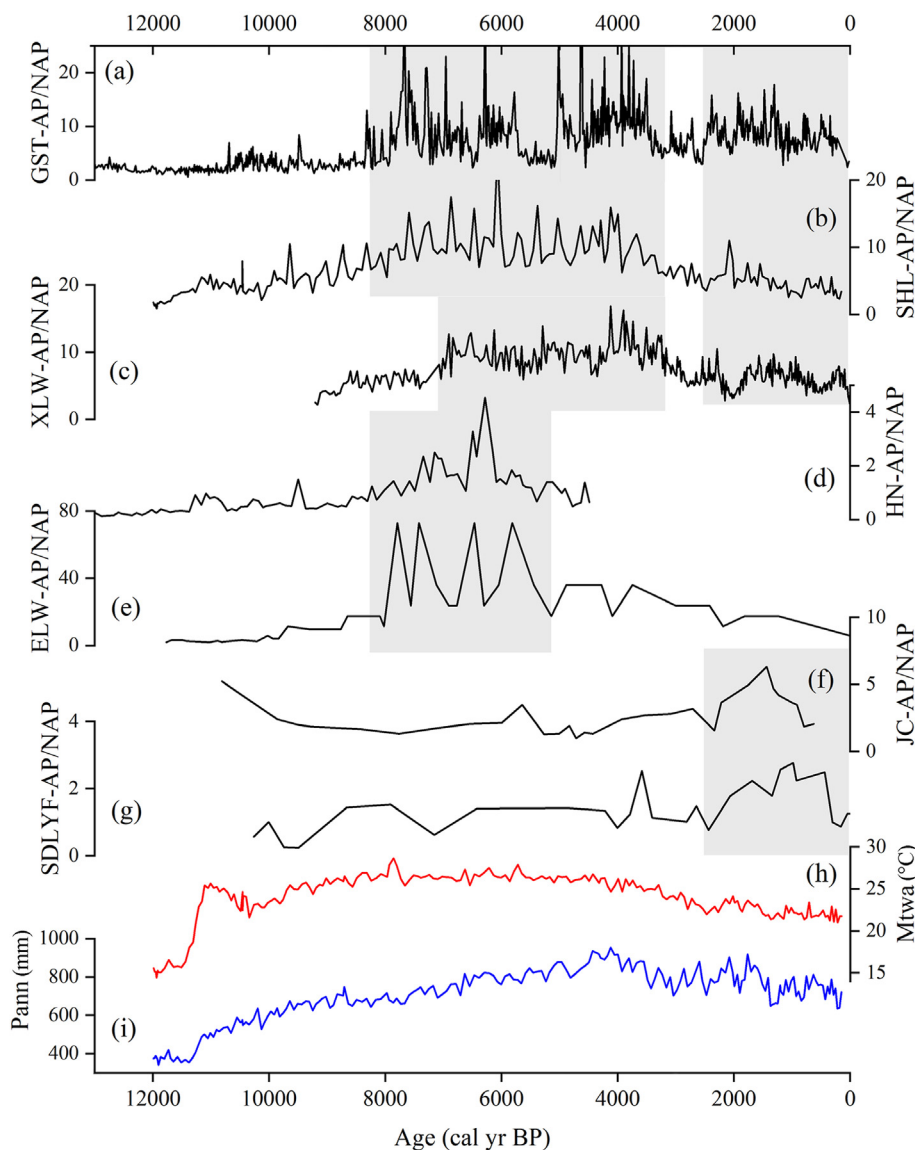
Fig. 6. The comparison of the ratio of arboreal to non-arboreal (AP/NAP) pollen and climate in Changbai Mountains. (**a**) This study; (**b**) Sihailongwan Maar Lake (SHL) (Stebich et al., 2015); (**c**) Xiaolongwan Maar Lake (XLW) (Xu et al., 2019); (**d**) Hani peatland (HN) (Yu et al., 2008); (**e**) Erlongwan Maar Lake (ELW) (Liu et al., 2009); (**f**) Jinchuan peatland (JC) (Jiang et al., 2008); (**g**) Sandaolaoyefu peatland (SDLYF) (Yuan and Sun, 1990); (**h**) mean temperature of the warmest month (Mtwa, °C) and (**i**) mean annual precipitation (Pann, mm) reconstructed from the SHL pollen record (Stebich et al., 2015). Grey boxes are the periods of significant increase in AP/NAP.

between Maat and Mtco (mean temperature of the coldest month) (coefficient = 0.43, $p \leq 0.01$) suggesting that Maat might be used as an index for winter conditions which, in addition to summer warmth, have a strong impact on the distribution of trees (Harrison et al., 2010). However, orbitally-induced changes in insolation during the Holocene resulted in increased summer temperatures and reduced winter temperatures in the northern latitudes during the early and middle Holocene (see e.g. Brierley et al., 2020) and this change in temperature seasonality means it is unlikely that modern-day correlations between Maat and Mtco would be preserved. We therefore focused on using climate reconstructions, specifically Mtwa and Pann, from the nearby SHL site.

According to our analyses, CHAR and fire frequency have an independent influence on forest composition on the multi-decadal timescale. However, there is no relationship with the inferred fire magnitude, either when CHAR is included in the analysis or when it is removed. Modern studies in northeast China indicate that forests recover within ~40–50 years even after severe fires (Cai et al., 2013), which is consistent with the lack of a relationship between fire magnitude and forest composition in our analyses. Furthermore, except during the early Holocene, high-magnitude fire events usually occur infrequently and thus fire frequency is low. The importance of fire frequency on forest composition reflects the fact that tolerance thresholds of individual species are exceeded when fire return times are shorter than the time needed for

seed production for individual species (Buhk et al., 2007) which in turn limits regrowth (Kuuluvainen et al., 2017; Turner et al., 2019). The negative impact of fire frequency is strongest for *Tilia* and *Ulmus* and has a smaller impact on *Betula*, which is consistent with the fact that *Betula* is faster growing and produces viable seed within a relatively short time (Hynynen et al., 2010). *Betula* can also recover quickly after fire because it typically has a large soil seed bank and can also resprout from the base after low intensity fires (Masaka et al., 2000; Tiebel, 2021). Despite the fact that the characteristic pine species in this region shows no particular adaptations to fire (McGregor et al., 2012), *Pinus* was the only taxon that displayed a positive relationship between fire frequency and abundance. This is consistent with the fact that this taxon is not particularly shade tolerant and seed germination success is strongly dependent on light levels (Zhang et al., 2015), so it benefits from frequent fires which provide more opportunities for successful regeneration through creating more open conditions. Changes in fire regime properties can be caused by multiple factors, including climate, vegetation characteristics, volcanic events and human activities; there is insufficient information to attribute the observed changes in fire regime at the GST site during the Holocene to any specific cause.

On the multi-decadal to centennial timescale examined here, climate has a greater effect than fires on forest openness and composition. This is perhaps not surprising, given that fires are short-lived events and

regrowth could occur within a matter of decades provided climate conditions were suitable. This also helps to explain why fire magnitude is unimportant whereas fire frequency or CHAR are related to changes in the abundance of most taxa. Intervals of higher fire frequency, or increased background levels of fire which also imply more frequent fires, have a deleterious effect on abundance because the recovery time between fires is shorter.

The pairwise correlation matrix showed that fire frequency and precipitation are significantly negatively correlated (Fig. 3), which suggests that climate can also indirectly affect forests by influencing fire. We hypothesize that forest resilience will face greater challenges when forests are subject to the overlapping effects of climate and fire, especially when there are large changes in drivers. The transformation of the forest state between 11.5 and 10.0 cal kyr BP, when *Ulmus* declined significantly and there were large expansions in *Quercus*, *Juglans*, *Tilia*, and *Pinus*, supports this view since this was a time characterised by both large climate changes and frequent severe fires leading to a reorganization of the system into a new ecological state (Millar and Stephenson, 2015; Turner et al., 2019; Baltzer et al., 2021).

5. Conclusions

Summer temperature, annual precipitation, the background level of fire and fire frequency have independent effects on forest openness and composition in the Changbai Mountains on decadal-to-centennial timescales. Summer temperature is the most important determinant of changes in the abundance of different taxa, with warmth-demanding broadleaf taxa showing predictable positive relationships and cold-tolerant conifers predictable negative relationships. While the influence of climate is stronger than that of fire on these timescales, intervals of increased fire frequency have a marked impact on forest composition because forest taxa that are less adapted to frequent fires have insufficient time to recover. However, the magnitude of the fires is unimportant for forest composition on these timescales, suggesting that frequency is more important than magnitude in determining forest resilience to disturbance.

Funding

Availability of date and materials

All data generated or analysed during this study are included in the article and its supplementary information files.

Authors' contributions

MM, SPH, DJ designed the study. MM, NL, BL, DL, GG and HN performed the field and laboratory experiments and pollen data analysis. DJ acquired funding. MM performed the analyses, and produced the Figures and Tables. MM and SPH wrote the original draft; all authors contributed to the final version.

Conflict of interests

The authors declare that they have no known competing financial interests or personal relationships that could have appeared to influence the work reported in this paper.

Acknowledgements

Appendix A. Supplementary data

Supplementary data to this article can be found online at https://doi.org/10.1016/j.fecs.2023.100127.

References

Andrus, R.A., Droske, C.A., Franz, M.C., Hudak, A.T., Lentile, L.B., Lewis, S.A., Morgan, P., Robichaud, P.R., Meddens, A.J., 2022. Spatial and temporal drivers of post-fire tree establishment and height growth in a managed forest landscape. Fire Ecol 18, 29.

Baltzer, J.L., Day, N.J., Walker, X.J., Greene, D., Mack, M.C., Alexander, H.D., Arseneault, D., Barnes, J.L., Bergeron, Y., Boucher, Y., Bourgeau-Chavez, L.L., Brown, C.D., Carriére, S., Howard, B.K., Gauthier, S., Parisien, M., Reid, K.A., Rogers, B.M., Roland, C.A., Sirois, L., Stehn, S.E., Thompson, D.K., Turetsky, M.R., Veraverbeke, S., Whitman, E., Yang, J., Johnstone, J.F., 2021. Increasing fire and the decline of fire adapted black spruce in the boreal forest. Proc. Natl. Acad. Sci. USA 118 (45), e2024872118.

Bartlein, P.J., Harrison, S.P., Brewer, S.C., Connor, S.C., Davis, B., Gajewski, K., Guiot, J., Harrison-Prentice, T., Henderson, A.K., Peyron, O., Prentice, I.C., Scholze, M., Seppä, H., Shuman, B.N., Sugita, S., Thompson, R.S., Viau, A.E., Williams, J., Wu, H., 2011. Pollen-based continental climate reconstructions at 6 and 21 ka: a global synthesis. Clim. Dynam. 37, 775–802.

Bistinas, I., Harrison, S.P., Prentice, I.C., Pereira, J.M.C., 2014. Causal relationships versus emergent patterns in the global controls of fire frequency. Biogeosciences 11, 5087–5101.

Blaauw, M., Christen, J.A., 2011. Flexible paleoclimate age-depth models using an autoregressive gamma process. Bayesian Anal 6, 457–474.

Bond, W.J., Woodward, F.I., Midgley, G.F., 2005. The global distribution of ecosystems in a world without fire. New Phytol. 165, 525–538.

Bowman, D.M., Balch, J.K., Artaxo, P., Bond, W.J., Carlson, J.M., Cochrane, M.A., D'Antonio, C.M., DeFries, R.S., Doyle, J.C., Harrison, S.P., Johnston, F.H., Keeley, J.E., Krawchuk, M.A., Kull, C.A., Marston, J., Moritz, M.A., Prentice, I.C., Roos, C.I., Scott, A.C., Swetnam, T.W., van der Werf, G.R., Pyne, S.J., 2009. Fire in the earth system. Science 324, 481–484.

Brierley, C.M., Zhao, A., Harrison, S.P., Braconnot, P., Williams, C.J.R., Thornalley, D.J.R., Shi, X., Peterschmitt, J.Y., Ohgaito, R., Kaufman, D.S., Kageyama, M., Hargreaves, J.C., Erb, M.P., Emile-Geay, J., D'Agostino, R., Chandan, D., Carré, M., Bartlein, P.J., Zheng, W., Zhang, Z., Zhang, Q., Yang, H., Volodin, E.M., Tomas, R.A., Routson, C., Peltier, W.R., Otto-Bliesner, B., Morozova, P.A., McKay, N.P., Lohmann, G., Legrande, A.N., Guo, C., Cao, J., Brady, E., Annan, J.D., Abe-Ouchi, A., 2020. Large-scale features and evaluation of the PMIP4-CMIP6 *midHolocene* simulations. Clim. Past 16, 1847–1872.

Buhk, C., Meyn, A., Jentsch, A., 2007. The challenge of plant regeneration after fire in the Mediterranean Basin: scientific gaps in our knowledge on plant strategies and evolution of traits. Plant Ecol. 192, 1–19.

Cai, W., Yang, J., Liu, Z., Hu, Y., Weisberg, P.J., 2013. Post-fire tree recruitment of a boreal larch forest in Northeast China. For. Ecol. Manag. 307, 20–29.

Chen, W., Moriya, K., Sakai, T., Koyama, L.A., Cao, C., 2014. Post-fire forest regeneration under different restoration treatments in the Greater Hinggan Mountain area of China. Ecol. Eng. 70, 304–311.

Connor, S.C., Ross, S.A., Sobotková, A., Herries, A.I., Mooney, S.D., Longford, C., Iliev, I.K., 2013. Environmental conditions in the SE balkans since the last glacial maximum and their influence on the spread of agriculture into europe. Quat. Sci. Rev. 68, 200–215.

Elvira, N.J., Lloret, F., Jaime, L., Margalef-Marrase, J., Pérez Navarro, M.Á., Batllori, E., 2021. Species climatic niche explains post-fire regeneration of Aleppo pine (*Pinus halepensis* Mill.) under compounded effects of fire and drought in east Spain. Sci. Total Environ. 798, 149308.

Faegri, K., Iversen, J., 1989. Textbook of Pollen Analysis, 4th. John Wiley & Sons, Chichester, New York, Brisbane, Toronto, Singapore.

Favre, É., Escarguel, G., Suc, J., Vidal, G., Thévenod, L., 2008. A contribution to deciphering the meaning of AP/NAP with respect to vegetation cover. Rev. Palaeobot. Palynol. 148, 13–35.

Fry, D.L., Stephens, S.L., 2006. Influence of humans and climate on the fire history of a ponderosa pine-mixed conifer forest in the southeastern Klamath Mountains, California. For. Ecol. Manag. 223, 428–438.

Gao, G., Jie, D., Li, D., Li, N., Liu, L., Liu, H., Shi, J., Leng, C., Wang, J., Liu, B., Li, P., 2018. Reliability of phytoliths for reconstructing vegetation dynamics in northern temperate forest regions: a case study in northeast China. Quat. Sci. Rev. 201, 1–12.

Hagmann, R.K., Hessburg, P.F., Salter, R.B., Merschel, A.G., Reilly, M.J., 2022. Contemporary wildfires further degrade resistance and resilience of fire-excluded forests. For. Ecol. Manag. 506, 119975.

Harrison, S.P., Bartlein, P.J., Brovkin, V.A., Houweling, S., Kloster, S., Prentice, I.C., 2018. The biomass burning contribution to climate–carbon-cycle feedback. Earth Syst. Dyn. 9, 663–677.

Harrison, S.P., Marlon, J.R., Bartlein, P.J., 2010. Fire in the earth system. In: Dodson, J. (Ed.), Changing Climates, Earth Systems and Society. Springer-Verlag, Amsterdam, pp. 21–48.

Harrison, S.P., Prentice, I.C., Bloomfield, K.J., Dong, N., Forkel, M., Forrest, M., Ningthoujam, R.K., Pellegrini, A.F., Shen, Y., Baudena, M., Cardoso, A.W., Huss, J.C., Joshi, J., Oliveras, I., Pausas, J.G., Simpson, K.J., 2021. Understanding and modelling wildfire regimes: an ecological perspective. Environ. Res. Lett. 16, 125008.

Haas, O., Prentice, I.C., Harrison, S.P., 2022. Global environmental controls on wildfire burnt area, size, and intensity. Environ. Res. Lett. 17, 065004.

Higuera, P.E., Brubaker, L.B., Anderson, P.M., Hu, F.S., Brown, T.A., 2009. Vegetation mediated the impacts of postglacial climate change on fire regimes in the south-central Brooks Range, Alaska. Ecol. Monogr. 79, 201–219.

Higuera, P.E., Briles, C.E., Whitlock, C., 2014. Fire-regime complacency and sensitivity to centennial-through millennial-scale climate change in Rocky Mountain subalpine forests, Colorado, USA. J. Ecol. 102, 1429–1441.

Hisano, M., Searle, E., Chen, H.Y., 2018. Biodiversity as a solution to mitigate climate change impacts on the functioning of forest ecosystems. Biol. Rev. 93, 439–456.

Hynynen, J., Niemistö, P., Viherä-Aarnio, A., Brunner, A., Hein, S., Velling, P., 2010. Silviculture of birch (*Betula pendula* roth and *Betula pubescens* ehrh.) in northern europe. Forestry 83, 103–119.

James, G., Witten, D., Hastie, T., Tibshirani, R., 2013. An Introduction to Statistical Learning: with Applications in R. Springer, New York.

Jiang, W., Leroy, S.A., Ogle, N., Chu, G., Wang, L., Liu, J., 2008. Natural and anthropogenic forest fires recorded in the Holocene pollen record from a Jinchuan peat bog, northeastern China. Palaeogeogr. Palaeoclimatol. Palaeoecol. 261, 47–57.

Kulakowski, D., Seidl, R., Holeksa, J., Kuuluvainen, T., Nagel, T.A., Panayotov, M., Svoboda, M., Thorn, S., Vacchiano, G., Whitlock, C., Wohlgemuth, T., Bebi, P., 2017. A walk on the wild side: disturbance dynamics and the conservation and management of European mountain forest ecosystems. For. Ecol. Manag. 388, 120–131.

Kuuluvainen, T., Hofgaard, A., Aakala, T., Jonsson, B.G., 2017. North Fennoscandian mountain forests: history, composition, disturbance dynamics and the unpredictable future. For. Ecol. Manag. 385, 140–149.

Kuneš, P., Svobodová-Svitavská, H., Kolář, J., Hajnalová, M., Abraham, V., Macek, M., Tkáč, P., Szabó, P., 2015. The origin of grasslands in the temperate forest zone of east-central Europe: long-term legacy of climate and human impact. Quat. Sci. Rev. 116, 15–27.

Larsen, W.A., McCleary, S.J., 1972. The use of partial residual plots in regression analysis. Technometrics 14, 781–790.

Li, J.D., Wu, B.H., Sheng, L.X., 2001. Jilin Vegetation. Jilin Science and Technology Press, Changchun (in Chinese).

Li, J., Yan, H., Dodson, J., Xu, Q., Sun, A., Cheng, B., Li, C., Ni, J., Zhang, X., Lu, F., 2018. Regional-scale precipitation anomalies in northern China during the Holocene and possible impact on prehistoric demographic changes. Geophys. Res. Lett. 45, 12477–12486.

Li, N.N., Chambers, F.M., Yang, J.X., Jie, D.M., Liu, L.D., Liu, H.Y., Gao, G.Z., Gao, Z., Li, D.H., Shi, J.C., Feng, Y.Y., Qiao, Z.H., 2017. Records of East Asian monsoon activities in Northeastern China since 15.6 ka, based on grain size analysis of peaty sediments in the Changbai Mountains. Quat. Int. 447, 158–169.

Liu, J., Chen, J., Zhang, X., Li, Y., Rao, Z., Chen, F., 2015. Holocene East Asian summer monsoon records in northern China and their inconsistency with Chinese stalagmite δ^{18}O records. Earth Sci. Rev. 148, 194–208.

Liu, J.L., 1989. Vegetational and climatic changes at Gushantun bog in Jilin, NE China since 13000 Y. BP. Acta Palaeontol. Sin. 28, 495–511 (in Chinese).

Liu, Y.Y., Liu, J.Q., Han, J.T., 2009. Pollen record and climate changing since 12.0 ka B.P. In erlongwan Maar Lake, Jilin Province. J. Jilin Univ. (Earth Sci. Ed.) 39, 93–98 (in Chinese).

Lusk, C.H., Clearwater, M.J., Laughlin, D.C., Harrison, S.P., Prentice, I.C., Nordenstahl, M., Smith, B., 2018. Frost and leaf-size gradients in forests: global patterns and experimental evidence. New Phytol. 219 (2), 565–573.

Masaka, K., Ohno, Y., Yamada, K., 2000. Fire tolerance and the fire-related sprouting characteristics of two cool-temperate broad-leaved tree species. Ann. Bot. 85, 137–142.

McFadden, D.L., 1974. Conditional logit analysis of qualitative choice behavior. Chapter 4. In: Zarembka, P. (Ed.), Frontiers in Econometrics. Academic Press Inc, New York, pp. 105–142.

McCullagh, P., Nelder, J.A., 1989. Generalized Linear Models, second ed. Chapman and Hall, New York.

McGregor, K.F., Watt, M.S., Hulme, P.E., Duncan, R.P., 2012. What determines pine naturalization: species traits, climate suitability or forestry use? Divers. Distrib 18, 1013–1023.

Meng, M., Jie, D., Li, D., Li, N., Liu, B., Gao, G., Wang, J., Niu, H., Liu, Y., Zhang, G., 2020. Fire history and its drivers based on peatland charcoal analysis in the Changbai Mountains, north-east China, during the last 13 000 years. Int. J. Wildland Fire 29, 841–854.

Millar, C.I., Stephenson, N.L., 2015. Temperate forest health in an era of emerging megadisturbance. Science 349, 823–826.

North, M., Tompkins, R.E., Bernal, A.A., Collins, B.M., Stephens, S.L., York, R.A., 2022. Operational resilience in western US frequent-fire forests. For. Ecol. Manag. 507, 120004.

O'Brien, R.M., 2007. A caution regarding rules of thumb for variance inflation factors. Qual. Quantity 41, 673–690.

Origin, 2022. OriginLab Corporation, Northampton, MA, USA.

Paulson, A.K., Pena, H., Alexander, H.D., Davydov, S., Loranty, M.M., Mack, M.C., Natali, S.M., 2021. Understory plant diversity and composition across a postfire tree density gradient in a Siberian Arctic boreal forest. Can. J. For. Res. 51, 720–731.

Power, M.J., Marlon, J.R., Ortiz, N., Bartlein, P.J., Harrison, S.P., Mayle, F.E., Ballouche, A., Bradshaw, R.H., Carcaillet, C., Córdova, C., Mooney, S., Moreno, P.I., Prentice, I.C., Thonicke, K., Tinner, W., Whitlock, C., Zhang, Y., Zhao, Y., Ali, A.A., Anderson, R.S., Beer, R., Behling, H., Briles, C.E., Brown, K.J., Brunelle, A.R.,

Bush, M.B., Camill, P., Chu, G., Clark, J.S., Colombaroli, D., Connor, S.C., Daniau, A., Daniels, M.L., Dodson, J., Doughty, E.D., Edwards, M.E., Finsinger, W., Foster, D., Frechette, J.D., Gaillard, M., Gavin, D.G., Gobet, E., Haberle, S.G., Hallett, D.J., Higuera, P.E., Hope, G., Horn, S., Inoue, J., Kaltenrieder, P., Kennedy, L.M., Kong, Z.C., Larsen, C., Long, C.J., Lynch, J.A., Lynch, E.A., McGlone, M.S., Meeks, S., Mensing, S.A., Meyer, G.D., Minckley, T.A., Mohr, J.A., Nelson, D.M., New, J., Newnham, R.M., Noti, R., Oswald, W.W., Pierce, J.R., Richard, P.J., Rowe, C., Sánchez Goñi, M.F., Shuman, B.N., Takahara, H., Toney, J.L., Turney, C.S., Urrego-Sanchez, D.H., Umbanhowar, C.E., Vandergoes, M., Vannière, B., Vescovi, E., Walsh, M., Wang, X., Williams, J.N., Wilmshurst, J.M., Zhang, J.H., 2008. Changes in fire regimes since the Last Glacial Maximum: an assessment based on a global synthesis and analysis of charcoal data. Clim. Dynam. 30, 887–907.

Prentice, I.C., 2010. The burning issue. Science 330, 1636–1637.

Qian, H., Yuan, X., Chou, Y., 2003. Forest vegetation of northeast China. Chapter 6. In: Kolbek, J., Šrůtek, M., Box, E.O. (Eds.), Forest Vegetation of Northeast Asia. Kluwer Academic Publishers, Dordrecht, pp. 181–230.

R Core Team, 2022. R: a Language and Environment for Statistical Computing. R Foundation for Statistical Computing, Vienna, Austria. https://www.R-project.org/. (Accessed 15 June 2023).

Reimer, P., Austin, W., Bard, E., Bayliss, A., Blackwell, P., Bronk Ramsey, C., Butzin, M., Cheng, H., Edwards, R.L., Friedrich, M., Grootes, P.M., Guilderson, T.P., Hajdas, I., Heaton, T.J., Hogg, A.G., Hughen, K.A., Kromer, B., Manning, S.W., Muscheler, R., Palmer, J.G., Pearson, C., van der Plicht, J., Reimer, R.W., Richards, D.A., Scott, E.M., Southon, J.R., Turney, C.S.M., Wacker, L., Adolphi, F., Büntgen, U., Capano, M., Fahrni, S., Fogtmann-Schulz, A., Friedrich, R., Köhler, P., Kudsk, S., Miyake, F., Olsen, J., Reinig, F., Sakamoto, M., Sookdeo, A., Talamo, S., 2020. The IntCal20 northern hemisphere radiocarbon age calibration curve (0–55 cal kBP). Radiocarbon 62 (4), 725–757.

Scheper, A., Verweij, P.A., Van Kuijk, M., 2021. Post-fire forest restoration in the humid tropics: a synthesis of available strategies and knowledge gaps for effective restoration. Sci. Total Environ. 771, 144647.

Searle, E.B., Chen, H.Y., 2017. Persistent and pervasive compositional shifts of western boreal forest plots in Canada. Global Change Biol. 23, 857–866.

Seidl, R., Thom, D., Kautz, M., Martin-Benito, D., Peltoniemi, M., Vacchiano, G., Wild, J., Ascoli, D., Petr, M., Honkaniemi, J., Lexer, M.J., Trotsiuk, V., Mairota, P., Svoboda, M., Fabrika, M., Nagel, T.A., Reyer, C.P., 2017. Forest disturbances under climate change. Nat. Clim. Change 7, 395–402.

Shi, G., Yan, H., Zhang, W., Dodson, J., Heijnis, H., Burrows, M., 2021. Rapid warming has resulted in more wildfires in northeastern Australia. Sci. Total Environ. 771, 144888.

Stebich, M., Mingram, J., Han, J., Liu, J., 2009. Late Pleistocene spread of (cool-) temperate forests in Northeast China and climate changes synchronous with the North Atlantic region. Global Planet. Change 65, 56–70.

Stebich, M., Rehfeld, K., Schlütz, F., Tarasov, P.E., Liu, J., Mingram, J., 2015. Holocene vegetation and climate dynamics of NE China based on the pollen record from Sihailongwan Maar Lake. Quat. Sci. Rev. 124, 275–289.

Stuiver, M., Reimer, P.J., 1993. Extended ^{14}C database and revised CALIB radiocarbon calibration program. Radiocarbon 35, 215–230.

Sweeney, L., Harrison, S.P., Linden, M.V., 2022. Assessing anthropogenic influence on fire history during the Holocene in the Iberian Peninsula. Quat. Sci. Rev. 287, 107562.

Tiebel, K., 2021. Which factors influence the density of birch (*Betula pendula* Roth) seeds in soil seed banks in temperate woodlands? Eur. J. For. Res. 140, 1441–1455.

Turner, M.G., Braziunas, K.H., Hansen, W.D., Harvey, B.J., 2019. Short-interval severe fire erodes the resilience of subalpine lodgepole pine forests. Proc. Natl. Acad. Sci. U.S.A. 116, 11319–11328.

Wang, F.X., Qian, N.F., Zhang, Y.L., Yang, H.Q., 1995. Pollen Flora of China. Science Press, Beijing, p. 461 (In Chinese).

Wang, X., Zhao, C., Jia, Q., 2013. Impacts of climate change on forest ecosystems in Northeast China. Adv. Clim. Change Res. 4, 230–241.

Willig, M.R., Presley, S.J., 2018. Biodiversity and disturbance. In: DellaSala, D.A., Goldstein, M.I. (Eds.), The Encyclopedia of the Anthropocene. Elsevier, pp. 45–51.

Xi, Y., Ning, J., 1994. Study on pollen morphology of plants from dry and semidry area in China. Yunshania 11, 119–191.

Xu, D., Lu, H., Chu, G., Liu, L., Shen, C., Li, F., Wang, C., Wu, N., 2019. Synchronous 500-year oscillations of monsoon climate and human activity in Northeast Asia. Nat. Commun. 10, 4105.

Xu, D., Lu, H., Chu, G., Wu, N., 2014. 500-year climate cycles stacking of recent centennial warming documented in an East Asian pollen record. Sci. Rep. 4, 3611.

Yang, X., Zhou, B., Xu, Y., Han, Z., 2021. CMIP6 evaluation and projection of temperature and precipitation over China. Adv. Atmos. Sci. 38, 817–830.

Yuan, S.M., Sun, X.J., 1990. The vegetational and environmental history at the west foot of Changbai Mountain, Northeast China during the last 10,000 years. Acta Bot. Sin. 32, 558–567 (in Chinese).

Yu, C.X., Luo, Y.L., Sun, X.J., 2008. A high-resolution pollen records from Hani Lake, Jilin, Northeast China showing climate changes between 13.1 cal. ka B.P. and 4.5 cal. ka B.P. Quat. Sci. 28, 929–938 (in Chinese).

Zhang, M., Yan, Q., Zhu, J., 2015. Optimum light transmittance for seed germination and early seedling recruitment of *Pinus koraiensis*: implications for natural regeneration. iForest 8, 853–859.

Zhang, S.R., 2015. Climate-vegetation Changes and Human Activities History of Gonghai Lake in Shanxi Province during Last 2000 Years. Master's Degree Thesis. Hebei Normal University, Shijiazhuang Province (in Chinese).

Zheng, Y., Pancost, R.D., Naafs, B.D., Li, Q., Liu, Z., Yang, H., 2018. Transition from a warm and dry to a cold and wet climate in NE China across the Holocene. Earth Planet Sci. Lett. 493, 36–46.

Zheng, Z., Huang, K., Xu, Q., Lu, H., Cheddadi, R., Luo, Y., Beaudouin, C., Luo, C., Zheng, Y., Li, C., Wei, J., Du, C., 2008. Comparison of climatic threshold of geographical distribution between dominant plants and surface pollen in China. Sci. China Earth Sci. 51, 1107–1120.

Zhou, X., Sun, L., Zhan, T., Huang, W., Zhou, X., Hao, Q., Wang, Y., He, X., Zhao, C., Zhang, J., Qiao, Y., Ge, J., Yan, P., Yan, Q., Shao, D., Chu, Z., Yang, W., Smol, J.P., 2016. Time-transgressive onset of the Holocene optimum in the East Asian monsoon region. Earth Planet Sci. Lett. 456, 39–46.

Zhu, H., Jiang, Z., Li, L.Z., 2021. Projection of climate extremes in China, an incremental exercise from CMIP5 to CMIP6. Sci. Bull. 66, 2528–2537.